JACS
JOURNAL OF THE AMERICAN CHEMICAL SOCIETY

Communication

pubs.acs.org/JACS

Nanoscale Molecular Traps and Dams for Ultrafast Protein Enrichment in High-Conductivity Buffers

Kuo-Tang Liao[†,‡] and Chia-Fu Chou*[,†,⊥,∥]

[†]Institute of Physics, [‡]Institute of Molecular Biology, [⊥]Genomics Research Center, and [∥]Research Center for Applied Sciences, Academia Sinica, Taipei 11529, Taiwan

Supporting Information

ABSTRACT: We report a new approach, *molecular dam*, to enhance mass transport for protein enrichment in nanofluidic channels by nanoscale electrodeless dielectrophoresis under physiological buffer conditions. Dielectric nanoconstrictions down to 30 nm embedded in nanofluidic devices serve as field-focusing lenses capable of magnifying the applied field to 10^5-fold when combined with a micro- to nanofluidic step interface. With this strong field and the associated field gradient at the nanoconstrictions, proteins are enriched by the molecular damming effect faster than the trapping effect, to $>10^5$-fold in 20 s, orders of magnitude faster than most reported methods. Our study opens further possibilities of using nanoscale molecular dams in miniaturized sensing platforms for rapid and sensitive protein analysis and biomarker discovery, with potential applications in precipitation studies and protein crystallization and possible extensions to small-molecules enrichment or screening.

Miniaturized biosensors and bioanalytical systems promise to revolutionize the field of health care and personalized medicine in light of sample reduction, speed, and sensitivity.[1] However, mass transport has generally been recognized as a major limiting factor in the sensitivity and performance of miniaturized sensor platforms, in that miniaturization leads to penalties on passive transport of biomolecules to the sensor surface due to increased diffusion length from the bulk liquid or in the direction of the fluidic channels.[2] Further, for low-abundance protein analysis, sample enrichment is often regarded as the first prerequisite for high-resolution analysis, since chemical amplification methods are not readily available for proteins. These factors pose major challenges for early or acute disease diagnostics and biomarker discovery using micro- or nanoscale sensor platforms. We report a new method for rapid enrichment and mass transport of proteins based on electrodeless dielectrophoresis (eDEP)[3] using an array of insulating nanoconstrictions as molecular *traps* or *dams* (preferred implementation), depending on the corresponding dielectric response of the molecules. We show that nanoconstrictions, serving as *field lenses*, may enhance local electric field to ~10^5-fold over the applied ac field and the associated field gradient. As a result of this strong field at the nanoconstrictions, Alexa-488-labeled streptavidins (52.8 kDa, 5 nm in diameter) are enriched by the molecular damming effect to $>10^5$-fold in <20 s in high-conductivity physiological buffers, orders of magnitude faster than most reported methods.[4] Our study opens further possibilities of using nanoscale molecular dams in miniaturized platforms for sensitive protein analysis, biomarker discovery, precipitation studies, and protein crystallization.[5]

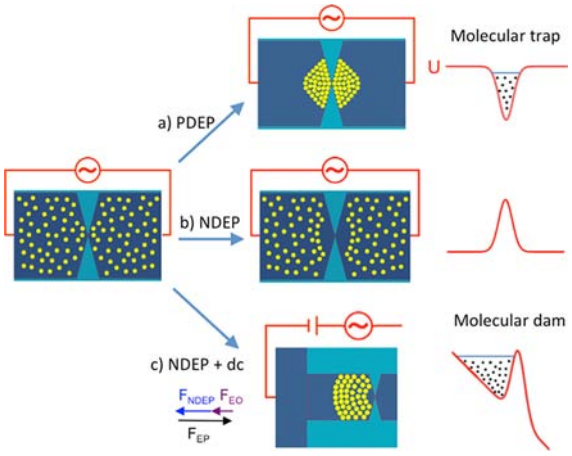

Figure 1. Concept of nanoscale molecular trap and dam. When an ac electric field is applied across an insulating nanoconstriction with a gap of tens of nm embedded in a sealed channel, the field can be highly focused, and a strong field gradient is generated for (a) *positive* dielectrophoresis (PDEP) or (b) *negative* dielectrophoresis (NDEP) if the dielectric permittivity of an analyte (shown in dots) is *larger* or *smaller* than that of the medium, respectively. The attractive potential in (a) serves as a *molecular trap*, while the repulsive potential in (b) keeps molecules away from the constriction. However, if a dc bias is applied in the case of NDEP, as shown in (c) for negatively charged particles, it tilts the repulsive potential into a slanted well, where the force balance condition, $F_{EP} = F_{EO} + F_{NDEP}$, occurs at local potential minimum, which could then cause protein accumulation in a continuous fashion, effectively working as a *molecular dam*.

Among the efforts for protein enrichment, electrokinetic methods using ion exclusion-enrichment effect by electrical double-layer (EDL) overlapping in a nanofluidic channel, or ion-selective permeable membranes such as Nafion, have been the most commonly adopted.[4a−h] Other methods based on conductivity gradient,[4j] temperature gradient,[4k−m] and patterned membranes[4n] for preconcentration have also been

Received: February 19, 2012
Published: May 17, 2012

dx.doi.org/10.1021/ja3016523 | *J. Am. Chem. Soc.* 2012, 134, 8742−8745

demonstrated. However, integrating sensing elements into these methods is not straightforward, since preconcentration is localized at the edges of the nanochannels. On the other hand, DEP[6] and the recently introduced eDEP,[3,7] or insulator-based dielectrophoresis (iDEP),[8] are known to be effective in the enrichment of DNA,[3,9] RNA,[10] viruses,[11] and cells[7,12] by exploiting the dielectric response of the bioparticles and its interaction with non-uniform electric fields. In particular, eDEP and its integration of DNA sensors demonstrated simultaneous sample enrichment and sensing.[13] However, recent reviews on eDEP cast doubts as to whether it could be implemented on chip for protein enrichment since either the size or the polarizability of proteins is much smaller than those of DNA or cells, and hence the demand for ultrahigh field gradient may not be easily realized.[14] In the current study, while we utilize highly focused fields at nanoconstrictions to enhance DEP forces, we alleviate problems associated with sensor integration by applying negative dielectrophoresis (NDEP) with dc bias; i.e., the net transport from electrophoresis (EP) is opposed by NDEP and electroosmosis (EO) through the force balance condition, $F_{EP} = F_{EO} + F_{NDEP}$, to enrich proteins away from the nanostructured points, a scheme we call a *molecular dam* (Figure 1). This scheme holds in general as long as the ac field imposes a strong NDEP scenario (ac field amplitude ≫ dc bias) at the constriction.

Classical DEP theory defines the translational force, i.e., the dielectrophoretic force, acting on a polarizable particle in a non-uniform field as $F_{DEP} = 2\pi r^3 \varepsilon_m Re[K(\omega)]\nabla E^2$, where r is the radius of the particle, ε_m the absolute permittivity of the suspending medium, E the amplitude of the applied field (i.e., root-mean-squared E in the case for an ac field), and $Re[K(\omega)]$ the real part of the Clausius−Mossotti (CM) factor, representing the frequency-dependent dielectric contrast between the particle and the suspending medium in an external driving field.[4h] It determines whether the particle transport is *toward*, when $Re[K(\omega)] > 0$, or *away from*, when $Re[K(\omega)] < 0$, the high field gradient region of the fluidic channel, correspondingly by *positive* dielectrophoresis (PDEP) or NDEP. The nanoscale molecular traps and dams implemented in this study are depicted in Figure 1.

Since F_{DEP} is proportional to the size of the molecules ($\sim r^3$), for proteins of few nanometers in size (~10—100 kDa) and small CM factor due to low polarizability, it is challenging within conventional devices to enrich proteins by DEP.[14] To overcome this issue, one needs to create a highly focused field and field gradient to enhance F_{DEP} by engineering the ∇E^2 (or $\mathbf{E}\cdot\nabla E$) term described above. The use of insulating nanoconstrictions provides both an enhanced field and field gradient to compensate the small size and low CM factor of the proteins, and to overcome its large diffusion coefficient. Based on this disposition, we have developed a fabrication process to construct eDEP nanoconstrictions embedded in nanofluidic channels (nanochannels) with interconnections to microfluidic channels for sample handling. (Device fabrication is detailed in the Supporting Information (SI).) To achieve nanoscale eDEP devices, fused silica was selected as the insulating substrate due to its robustness and low auto-fluorescence. The experimental layout and overall chip configuration are displayed in Figure 2a,b. Optical and scanning electron micrographs (Figure 2c,d) show that parallel nanochannels containing arrayed nanoconstriction structures may be constructed on one chip.

Due to the simple fact that the displacement current in a conducting buffer may be focused (or enhanced) by reducing of

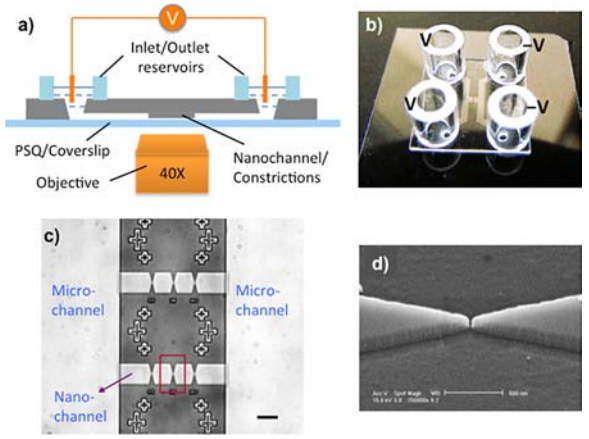

Figure 2. (a) Schematic of the experimental layout. Four Au electrodes are inserted into the reservoirs, shown in (b), where the electric field is applied. Experiments are monitored by an inverted fluorescence microscope via a 40× objective and an EMCCD (see Supporting Information). (b) Photograph of an assembled device (14×14 mm^2) made in fused silica (see Figure S1). The two reservoirs at each side of the H-shaped microchannel, 750 μm × 3 μm, are kept at equal potential. (c) Optical micrograph showing the center of the "H" where long nanofluidic channels (30 μm × 220 nm) are connected by microfluidic channels. Three nanoconstrictions are seeded in each of the five nanochannels (two shown here). (d) SEM image of the boxed nanoconstriction (viewed in 90° turn) in (c), with 30 nm gap size. Scale bar: (c) 30 μm; (d) 500 nm.

a cross-section of an insulating fluidic channel, it is straightforward to estimate the field-focusing factor in our device. If a microchannel with dimensions $X_{micro}\times Z_{micro}$ (width×height) is reduced to a nanochannel of $X_{nano}\times Z_{nano}$, and the nanochannel is further reduced to a nanoconstriction of width X_c, then from the continuity equation (current conservation) one can easily find the design rule for the overall field lens power to be $(X_{micro}/X_{nano})\times(Z_{micro}/Z_{nano})\times(X_{nano}/X_c)/n$, where n is the number of parallel nanochannels ($n = 5$ in our device), provided the conductivity of the buffer remains constant over all fluidic passages. This assumption is valid as the Debye screening length (<1 nm) in the buffers used in our experiments is much less than the nanoconstriction width and nanochannel height of our device. This condition is still far from the EDL overlapping scenario, where the concentration polarization effect is prounced.[4a−f] From our current design, the cross section of the microchannel is 750 μm × 3 μm^2, and that of the nanochannel is 30 μm × 220 nm, with nanoconstriction width 30 nm. The overall field-focusing factor is $\sim 7\times 10^4 X$, leading to an enhancement factor of $\sim 5\times 10^9$ for the dielectrophoretic force ($\sim E^2$) at the nanoconstrictions.[3,7] Empowered by such a strong enhancement of the field and field gradient, we were able to perform both PDEP and NDEP in our device using Alexa-488-labeled streptavidins as model proteins in physiological buffer conditions (10 mM phosphate-buffered saline with 150 mM NaCl, conductivity 1.6 S/m). Conversely, conventional metal electrode-based dielectrophoresis (MDEP) is not effective to overcome the strong EDL screening effect, due to the limitation of applied field strength, and hence could not easily polarize the protein−counterion cloud complex in high-salt conditions.[4a,c,h] On the other hand, the protein enrichment schemes using the co-ion depletion effect, caused by EDL overlapping, suffer from the relatively low

dx.doi.org/10.1021/ja3016523 | J. Am. Chem. Soc. 2012, 134, 8742−8745

potential barrier; hence, high dc bias cannot be applied for rapid protein accumulation.[4a−d,g,h]

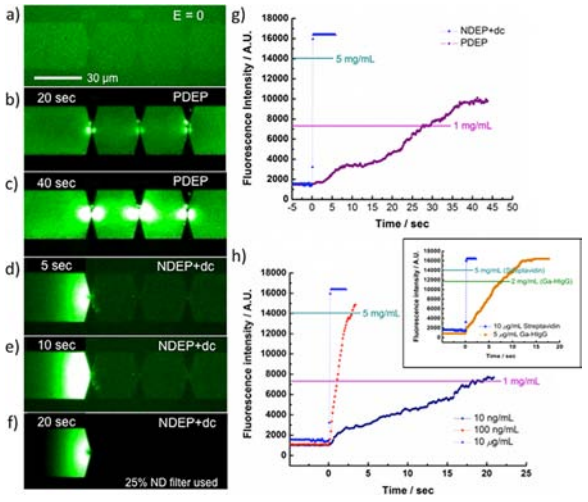

Figure 3. Protein trapping and damming with nanoscale eDEP. (a) Proteins (Alexa-488 streptavidins, 10 μg/mL) loaded in the chip by capillary force. Protein trapping with PDEP (b) 20 and (c) 40 s after 473 V_{pp}/cm ac field applied across the chip at 10 kHz. This field is focused 7×10^4-fold (~3.3×10^9 V_{pp}/m) over the applied field at the constrictions. All three constrictions show trapping of streptavidins, indicating PDEP is at work. (d−f) Protein damming demonstrated by NDEP+dc: ac field of 214 V_{pp}/cm is applied at 1 MHz with 1.5 V/cm dc bias (with positive potential at the right side of the channel). The image in (f) was taken with a 25% transmittance neutral density (ND) filter to keep the intensity below saturation of the EMCCD. The dark zone at the center of the first constriction indicates NDEP is at work where streptavidins are repelled. Virtually no excess molecules go beyond the first dam before reaching its saturation for effective accumulation at the second and third dams to show dark zones with good contrast. (g) Corresponding intensity plot of protein enrichment, at the same initial concentration of 10 μg/mL, under the same experimental conditions used for molecular trapping and damming. The plateau in the damming curve means the EMCCD has reached saturation (an extended intensity plot with the use of ND filter is shown in Figure S2). (h) Protein enrichment curves for various initial concentrations (10 ng/mL or 189 pM, 100 ng/mL, and 10 μg/mL) when operated under the molecular damming effect with corresponding dc bias of 1.5, 4.5, and 1.5 V/cm. The concentration rulers of streptavidin are drawn as horizontal lines. Note that 10 ng/mL proteins are enhanced >10^5-fold in <20 s. The inset shows the damming of goat anti-human IgG, which reaches 400-fold enrichment in 7.5 s from a concentration of 5 μg/mL (33 nM), against streptavidins (500-fold enrichment in <1 s) under the same applied field conditions as in (d−f).

Figure 3 summarizes our observation of the molecular trapping and damming effects through the operation of PDEP and NDEP with dc bias, respectively. Panels a−c demonstrate that PDEP for streptavidins may operate in arrayed nanoconstrictions and occurs at 10 kHz. However, when the frequency is increased to ~1 MHz, the DEP undergoes a crossover response from PDEP to NDEP with a changed sign of $K(\omega)$, consistent with other published results.[16] Panels d−f show the molecular damming effect for streptavidin enrichment when operated under NDEP with dc bias. These observations verify that the concepts depicted in Figure 1 are at work.

To compare the effectiveness of protein enrichment by PDEP (trapping) and NDEP with dc bias (damming), we loaded the chips with the same initial concentration of 10 μg/mL Alexa-488 streptavidins. Figure 3g indicates that the damming effect is much more efficient in protein enrichment, as 10^3-fold concentration enhancement may be achieved 2−3 s after the field is turned on, much faster than the trapping effect (see SI Figure S2 and Movies M1 and M2). In fact, this result suggests that, for practical applications, nanoscale eDEP as a molecular dam (NDEP+dc) is particularly advantageous for three reasons: it is much more effective in protein enrichment than PDEP; concerns of potential Joule heating effect are alleviated by displacement of the molecular dam away from the hot spot, i.e., the geometrical center of the nanoconstriction; and the sensing element can be placed micrometers away from the nanoconstriction, a task easily achievable by conventional photolithography. This circumvents the great technical challenge of integrating biosensors at the center or in the immediate proximity of the nanoconstrictions when operating in PDEP scheme.

To further characterize the enrichment factors for different initial protein concentrations under molecular damming conditions, streptavidins of 10 ng/mL, 100 ng/mL, and 10 μg/mL were loaded into the chips. Figure 3h shows the enrichment curves at various starting concentrations of streptavidin, where the concentration rulers of 1 and 5 mg/mL are drawn as horizontal lines under the same buffer conditions as those used in experiments to serve as references for calculating the enrichment factor and the time needed to reach the concentration rulers. To ensure the molecular damming strategy developed here is applicable to other proteins, we also tested Alexa-488-labeled goat anti-human IgG (~150 kDa, see SI) in comparison to Alexa-488 streptavidins (inset in Figure 3h). The results indicate the effect of the molecular size and the polarizability for different proteins. Note that all the data presented in Figure 3g,h and Figure S2 are plotted from the region of highest intensity of fluorescent signals (with an area of 9.6 μm^2 or 24 pixels) where proteins are mostly enriched, after subtracting the background from dark counts and auto-fluorescence from the substrate. Based on these results, a protein enrichment factor of >10^5-fold may be achieved in just seconds when operating in the damming scheme, orders of magnitude faster than most previous studies.[4a,c,h] We attribute the fast transport of molecules to the highly constricted field at both the micro- to nanochannel junction and the nanoconstriction. This is indeed a unique feature of our device. Streptavidin velocity is enhanced from ~1.5 μm/s in microchannel (1.5 V/cm applied dc bias and bulk mobility 0.8 ± 0.9 μm-cm/V-s)[4j] to ~100 μm/s by a 70-fold field enhancement when entering into the nanochannel, and further to ~10−15 cm/s by another 1000-fold field enhancement from the junction to the nanoconstriction (~45 μm distance). To estimate the effective potential energy U_{min} involved in the damming process using Boltzmann distribution, 10^5-fold concentration enrichment corresponds to $U_{min} \approx -12\ k_BT$, where k_BT is the thermal energy. Since in the experiments the system did not reach equilibrium as proteins kept accumulating during the process, this estimation would suggest a lower bound of the effective potential well.

To demonstrate that the balance of F_{EO} and F_{EP} alone cannot achieve the significant protein enrichment observed in our device, we studied the case of a pure dc field (up to 4.5 V/cm) but did not observe any discernible protein enrichment (see SI, Movie M3). In fact, it suggests F_{EP} is much higher than F_{EO} in our device. To further demonstrate the essential role of F_{NDEP}

dx.doi.org/10.1021/ja3016523 | J. Am. Chem. Soc. 2012, 134, 8742−8745

in molecular damming, we turned off the ac field but not the dc bias and observed the highly enriched proteins quickly diffusing away due to the concentration gradient established by the molecular dam (see SI, Movie M4). Hence, F_{NDEP} is essential for the protein damming effect in our design.

The potential Joule heating effect due to the highly focused field (total current 25 μA, or 5 μA/nanochannel) at the nanoconstrictions may be alleviated by the small sample volume (~1 pL/nanochannel), with a 220 nm liquid layer in the nanochannels, used in our devices. Hence heat dissipation through the substrate, as a bulk thermal bath, is very effective based on our previous study by finite-element multiphysics simulation.[13,17] Within our experimental conditions, we assume the proteins at the trap are not denatured, as the trapping events are reversible, and there is no denaturation-associated aggregation observed in our experiments. The issues discussed here are further assuaged if one operates the device as molecular dams where enriched proteins are away from the highly focused field constrictions.

Although protein trapping has been demonstrated using a 100-nm nanopipet with quasi-dc driving field,[18] and insulator post-array with dc field (iDEP with low-conductivity buffers to avoid Joule heating),[19] it remains challenging to detect ultra-low protein targets due to the limited protein enrichment factor achieved (up to 1000-fold) and to integrate it within a fluidic chip platform where multiplexing and parallel analysis are desirable (in the nanopipet approach). However, the concept of the molecular damming effect introduced in this study is exceedingly compatible with multiplexing, parallel analysis, and high-conductivity buffers, and thus suitable for integrating biosensors.

In summary, we present a nanoscale active molecular transport scheme for ultrafast protein enrichment by constructing nanoscale molecular traps and dams using electrodeless dielectrophoresis generated by insulating nano-constricted structures. A protein enrichment factor $>10^5$ has been achieved in <20 s, orders of magnitude faster than most of the reported methods. Multichannel layout for parallel operation has also been demonstrated. In this scenario, miniaturization alleviates rather than accentuates the transport limitations, so that any sensor applications can capitalize on the ultrafast sample enrichment schemes introduced here. Though our device could also be applied to DNA and RNA analysis,[3,10,13] it may find applications in general protein assays, protein crystallization, rare biomarker discovery (e.g., coupled with mass spectroscopy), and early disease diagnostics in lab-on-a-chip systems, with potential extensions to enrichment or screening of small molecules (e.g., peptides or carbohydrates).

■ ASSOCIATED CONTENT

Supporting Information

Details of device fabrication and protein enrichment; movies showing molecular trapping and damming effects. This material is available free of charge via the Internet at http://pubs.acs.org.

■ AUTHOR INFORMATION

Corresponding Author

cfchou@phys.sinica.edu.tw

Notes

The authors declare no competing financial interest.

■ ACKNOWLEDGMENTS

This work was supported by an AS Postdoctoral Fellowship (to KTL), AS Nano Program and Foresight Project (AS-97-FP-M02), NSC-Taiwan (99-2112-M-001-027-MY3), and USAF-AOARD (FA2386-12-1-4002). We thank Dr. Qi-Huo Wei for his early involvement of this project, Prof. N. S. Swami for critical comments on the manuscript, Drs. C. H. Lee and T. Leichle for helpful discussions, and AS Nano Core Facility.

■ REFERENCES

(1) (a) Vilkner, T.; Janasek, D.; Manz, A. *Anal. Chem.* **2004**, *76*, 3373. (b) Dittrich, P. S.; Manz, A. *Nat. Rev. Drug Discov.* **2006**, *5*, 210.

(2) (a) Nair, P. R.; Alam, M. A. *Appl. Phys. Lett.* **2006**, *88*, 233120. (b) Sparreboom, W.; van den Berg, A.; Eijkel, J. C. T. *Nat. Nanotech.* **2009**, *4*, 713. (c) Sheehan, P. E.; Whitman, L. J. *Nano Lett.* **2005**, *5*, 803. (d) Cohen, A. E.; Fields, A. P. *ACS Nano* **2011**, *5*, 5296.

(3) Chou, C.-F.; Tegenfeldt, J. O.; Bakajin, O.; Chan, S. S.; Cox, E. C.; Darnton, N.; Duke, T.; Austin, R. H. *Biophys. J.* **2002**, *83*, 2170.

(4) (a) Wang, Y.-C.; Stevens, A. L.; Han, J. *Anal. Chem.* **2005**, *77*, 4293. (b) Huang, H.; Xu, F.; Dai, Z.; Lin, B. *Electrophoresis* **2005**, *26*, 2254. (c) Kim, S. M.; Burns, M. A.; Hasselbrink, E. F. *Anal. Chem.* **2006**, *78*, 4779. (d) Armenta, J. M.; Gu, B.; Thulin, C. D.; Lee, M. L. *J. Chromatogr. A* **2007**, *1148*, 115. (e) Huang, K. D.; Yang, R. J. *Electrophoresis* **2008**, *29*, 4862. (f) Wu, D. P.; Steckl, A. J. *Lab Chip* **2009**, *9*, 1890. (g) Nie, F.-Q.; Macka, M.; Paull, B. *Lab Chip* **2007**, *7*, 1597. (h) Lee, J. H.; Song, Y.-A.; Han, J. *Lab Chip* **2008**, *8*, 596. (i) Greenlee, R. D.; Ivory, C. F. *Biotechnol. Prog.* **1998**, *14*, 300. (j) Inglis, D. W.; Goldys, E. M.; Calander, N. P. *Angew. Chem., Int. Ed.* **2011**, *50*, 7546. (k) Ross, D.; Locascio, L. E. *Anal. Chem.* **2002**, *74*, 2556. (l) Matsui, T.; Franzke, J.; Manz, A.; Janasek, D. *Electrophoresis* **2007**, *28*, 4606. (m) Ge, Z. W.; Wang, W.; Yang, C. *Lab Chip* **2011**, *11*, 1396. (n) Cheetham, M. R.; et al. *J. Am. Chem. Soc.* **2011**, *133*, 6521.

(5) Vilozny, B.; Actis, P.; Seger, R. A.; Pourmand, N. *ACS Nano* **2011**, *5*, 3191.

(6) Pethig, R. *Biomicrofluidics* **2010**, *4*, 022811.

(7) Chou, C.-F.; Zenhausern, F. *IEEE Eng. Med. Biol. Mag.* **2003**, *22*, 62.

(8) Cummings, E. B.; Singh, A. K. *Anal. Chem.* **2003**, *75*, 4724.

(9) Asbury, C. L.; van den Engh, G. *Biophys. J.* **1998**, *74*, 1024.

(10) Giraud, G.; et al. *Biomicrofluidics* **2011**, *5*, 024116.

(11) (a) Lapizco-Encinas, B. H.; Rito-Palomares, M. *Electrophoresis* **2007**, *28*, 4521. (b) Hughes, M. P.; Morgan, H.; Rixon, F. J.; Burt, J. P. H.; Pethig, R. *Biochim. Biophys. Acta* **1998**, *1425*, 119.

(12) (a) Pethig, R. *Crit. Rev. Biotechnol.* **1996**, *16*, 331. (b) Lapizco-Encinas, B. H.; Simmons, B. A.; Cummings, E. B.; Fintschenko, Y. *Anal. Chem.* **2004**, *76*, 1571.

(13) Swami, N.; Chou, C. F.; Ramamurthy, V.; Chaurey, V. *Lab Chip* **2009**, *9*, 3212.

(14) (a) Regtmeier, J.; Eichhorn, R.; Viefhues, M.; Bogunovic, L.; Anselmetti, D. *Electrophoresis* **2011**, *32*, 2253. (b) Srivastava, S. K.; Gencoglu, A.; Minerick, A. R. *Anal. Bioanal. Chem.* **2011**, *399*, 301.

(15) Pohl, H. A. *Dielectrophoresis: The Behavior of Neutral Matter in Nonuniform Electric Fields*; Cambridge University Press: Cambridge, 1978.

(16) (a) Gascoyne, P. R. C.; Vykoukal, J. *Electrophoresis* **2002**, *23*, 1973. (b) Hughes, M. P. *Electrophoresis* **2002**, *23*, 2569. (c) Basuray, S.; Chang, H.-C. *Phys. Rev. E* **2007**, *75*, 060501.

(17) Chaurey, V.; Polanco, C.; Chou, C. F.; Swami, N. S. *Biomicrofluidics* **2012**, *6*, 012806.

(18) Clarke, R. W.; White, S. S.; Zhou, D.; Ying, L.; Klenerman, D. *Angew. Chem., Int. Ed.* **2005**, *44*, 3747.

(19) Lapizco-Encinas, B. H.; Ozuna-Chacon, S.; Rito-Palomares, M. *J. Chromatogr. A* **2008**, *1206*, 45.